Determination of the LEP beam energy using radiative fermion-pair events

OPAL Collaboration

G. Abbiendi [b], C. Ainsley [e], P.F. Åkesson [c,23], G. Alexander [u], J. Allison [o], P. Amaral [h], G. Anagnostou [a], K.J. Anderson [h], S. Asai [v], D. Axen [z], I. Bailey [y], E. Barberio [g,15], T. Barillari [ae], R.J. Barlow [o], R.J. Batley [e], P. Bechtle [x], T. Behnke [x], K.W. Bell [s], P.J. Bell [a], G. Bella [u], A. Bellerive [f], G. Benelli [d], S. Bethke [ae], O. Biebel [ad], O. Boeriu [i], P. Bock [j], M. Boutemeur [ad], S. Braibant [b], R.M. Brown [s], H.J. Burckhart [g], S. Campana [d], P. Capiluppi [b], R.K. Carnegie [f], A.A. Carter [l], J.R. Carter [e], C.Y. Chang [p], D.G. Charlton [a], C. Ciocca [b], A. Csilling [ab], M. Cuffiani [b], S. Dado [t], A. De Roeck [g], E.A. De Wolf [g,18], K. Desch [x], B. Dienes [ac], M. Donkers [f], J. Dubbert [ad], E. Duchovni [w], G. Duckeck [ad], I.P. Duerdoth [o], E. Etzion [u], F. Fabbri [b], P. Ferrari [g], F. Fiedler [ad], I. Fleck [i], M. Ford [o], A. Frey [g], P. Gagnon [k], J.W. Gary [d], C. Geich-Gimbel [c], G. Giacomelli [b], P. Giacomelli [b], M. Giunta [d], J. Goldberg [t], E. Gross [w], J. Grunhaus [u], M. Gruwé [g], P.O. Günther [c], A. Gupta [h], C. Hajdu [ab], M. Hamann [x], G.G. Hanson [d], A. Harel [t], M. Hauschild [g], C.M. Hawkes [a], R. Hawkings [g], R.J. Hemingway [f], G. Herten [i], R.D. Heuer [x], J.C. Hill [e], K. Hoffman [h], D. Horváth [ab,3], P. Igo-Kemenes [j], K. Ishii [v], H. Jeremie [q], P. Jovanovic [a], T.R. Junk [f,8], J. Kanzaki [v,19], D. Karlen [y], K. Kawagoe [v], T. Kawamoto [v], R.K. Keeler [y], R.G. Kellogg [p], B.W. Kennedy [s], S. Kluth [ae], T. Kobayashi [v], M. Kobel [c], S. Komamiya [v], T. Krämer [x], P. Krieger [f,11], J. von Krogh [j], T. Kuhl [x], M. Kupper [w], G.D. Lafferty [o], H. Landsman [t], D. Lanske [m], D. Lellouch [w], J. Letts [14], L. Levinson [w], J. Lillich [i], S.L. Lloyd [l], F.K. Loebinger [o], J. Lu [z,21], A. Ludwig [c], J. Ludwig [i], W. Mader [c,2], S. Marcellini [b], A.J. Martin [l], G. Masetti [b], T. Mashimo [v], P. Mättig [12], J. McKenna [z], R.A. McPherson [y], F. Meijers [g], W. Menges [x], F.S. Merritt [h], H. Mes [f,1], N. Meyer [x], A. Michelini [b], S. Mihara [v], G. Mikenberg [w], D.J. Miller [n], W. Mohr [i], T. Mori [v], A. Mutter [i], K. Nagai [l], I. Nakamura [v,20], H. Nanjo [v], H.A. Neal [af], R. Nisius [ae], S.W. O'Neale [a,✠], A. Oh [g], M.J. Oreglia [h], S. Orito [v,✠], C. Pahl [ae], G. Pásztor [d,6], J.R. Pater [o], J.E. Pilcher [h], J. Pinfold [aa], D.E. Plane [g], O. Pooth [m], M. Przybycień [g,13], A. Quadt [c], K. Rabbertz [g,17], C. Rembser [g], P. Renkel [w],

J.M. Roney [y], A.M. Rossi [b], Y. Rozen [t], K. Runge [i], K. Sachs [f], T. Saeki [v],
E.K.G. Sarkisyan [g,9], A.D. Schaile [ad], O. Schaile [ad], P. Scharff-Hansen [g], J. Schieck [ae],
T. Schörner-Sadenius [g,24], M. Schröder [g], M. Schumacher [c], R. Seuster [m,5],
T.G. Shears [g,7], B.C. Shen [d], P. Sherwood [n], A. Skuja [p], A.M. Smith [g], R. Sobie [y],
S. Söldner-Rembold [o], F. Spano [h], A. Stahl [c,22], D. Strom [r], R. Ströhmer [ad], S. Tarem [t],
M. Tasevsky [g,18], R. Teuscher [h], M.A. Thomson [e], E. Torrence [r], D. Toya [v], P. Tran [d],
I. Trigger [g], Z. Trócsányi [ac,4], E. Tsur [u], M.F. Turner-Watson [a], I. Ueda [v], B. Ujvári [ac,4],
C.F. Vollmer [ad], P. Vannerem [i], R. Vértesi [ac,4], M. Verzocchi [p], H. Voss [g,16],
J. Vossebeld [g,7], C.P. Ward [e], D.R. Ward [e], P.M. Watkins [a], A.T. Watson [a], N.K. Watson [a],
P.S. Wells [g], T. Wengler [g], N. Wermes [c], G.W. Wilson [o,10], J.A. Wilson [a], G. Wolf [w],
T.R. Wyatt [o], S. Yamashita [v], D. Zer-Zion [d], L. Zivkovic [w]

[a] *School of Physics and Astronomy, University of Birmingham, Birmingham B15 2TT, UK*
[b] *Dipartimento di Fisica dell' Università di Bologna and INFN, I-40126 Bologna, Italy*
[c] *Physikalisches Institut, Universität Bonn, D-53115 Bonn, Germany*
[d] *Department of Physics, University of California, Riverside, CA 92521, USA*
[e] *Cavendish Laboratory, Cambridge CB3 0HE, UK*
[f] *Ottawa-Carleton Institute for Physics, Department of Physics, Carleton University, Ottawa, ON K1S 5B6, Canada*
[g] *CERN, European Organisation for Nuclear Research, CH-1211 Geneva 23, Switzerland*
[h] *Enrico Fermi Institute and Department of Physics, University of Chicago, Chicago, IL 60637, USA*
[i] *Fakultät für Physik, Albert-Ludwigs-Universität Freiburg, D-79104 Freiburg, Germany*
[j] *Physikalisches Institut, Universität Heidelberg, D-69120 Heidelberg, Germany*
[k] *Indiana University, Department of Physics, Bloomington, IN 47405, USA*
[l] *Queen Mary and Westfield College, University of London, London E1 4NS, UK*
[m] *Technische Hochschule Aachen, III Physikalisches Institut, Sommerfeldstrasse 26-28, D-52056 Aachen, Germany*
[n] *University College London, London WC1E 6BT, UK*
[o] *Department of Physics, Schuster Laboratory, The University, Manchester M13 9PL, UK*
[p] *Department of Physics, University of Maryland, College Park, MD 20742, USA*
[q] *Laboratoire de Physique Nucléaire, Université de Montréal, Montréal, PQ H3C 3J7, Canada*
[r] *University of Oregon, Department of Physics, Eugene, OR 97403, USA*
[s] *CCLRC Rutherford Appleton Laboratory, Chilton, Didcot, Oxfordshire OX11 0QX, UK*
[t] *Department of Physics, Technion-Israel Institute of Technology, Haifa 32000, Israel*
[u] *Department of Physics and Astronomy, Tel Aviv University, Tel Aviv 69978, Israel*
[v] *International Centre for Elementary Particle Physics and Department of Physics, University of Tokyo, Tokyo 113-0033,
and Kobe University, Kobe 657-8501, Japan*
[w] *Particle Physics Department, Weizmann Institute of Science, Rehovot 76100, Israel*
[x] *Universität Hamburg/DESY, Institut für Experimentalphysik, Notkestrasse 85, D-22607 Hamburg, Germany*
[y] *University of Victoria, Department of Physics, PO Box 3055, Victoria, BC V8W 3P6, Canada*
[z] *University of British Columbia, Department of Physics, Vancouver, BC V6T 1Z1, Canada*
[aa] *University of Alberta, Department of Physics, Edmonton, AB T6G 2J1, Canada*
[ab] *Research Institute for Particle and Nuclear Physics, PO Box 49, H-1525 Budapest, Hungary*
[ac] *Institute of Nuclear Research, PO Box 51, H-4001 Debrecen, Hungary*
[ad] *Ludwig-Maximilians-Universität München, Sektion Physik, Am Coulombwall 1, D-85748 Garching, Germany*
[ae] *Max-Planck-Institute für Physik, Föhringer Ring 6, D-80805 München, Germany*
[af] *Yale University, Department of Physics, New Haven, CT 06520, USA*

Editor: L. Rolandi

Abstract

We present a determination of the LEP beam energy using "radiative return" fermion-pair events recorded at centre-of-mass energies from 183 to 209 GeV. We find no evidence of a disagreement between the OPAL data and the LEP Energy Working Group's standard calibration. Including the energy-averaged 11 MeV uncertainty in the standard determination, the beam energy we obtain from the OPAL data is higher than that obtained from the LEP calibration by 0 ± 34(stat.) ± 27(syst.) MeV.

1. Introduction

The measurement of the mass of the W boson, M_W, is one of the principal goals of the LEP II program. The resolution on the measured W mass is greatly improved by employing kinematic fits, in which the

E-mail address: plane@cern.ch (D.E. Plane).

[1] And at TRIUMF, Vancouver, Canada V6T 2A3.

[2] Now at University of Iowa, Department of Physics and Astronomy, Iowa, USA.

[3] And Institute of Nuclear Research, Debrecen, Hungary.

[4] And Department of Experimental Physics, University of Debrecen, Hungary.

[5] And MPI München.

[6] And Research Institute for Particle and Nuclear Physics, Budapest, Hungary.

[7] Now at University of Liverpool, Department of Physics, Liverpool L69 3BX, UK.

[8] Now at Department Physics, University of Illinois at Urbana-Champaign, USA.

[9] And Manchester University.

[10] Now at University of Kansas, Department of Physics and Astronomy, Lawrence, KS 66045, USA.

[11] Now at University of Toronto, Department of Physics, Toronto, Canada.

[12] Current address Bergische Universität, Wuppertal, Germany.

[13] Now at University of Mining and Metallurgy, Cracow, Poland.

[14] Now at University of California, San Diego, USA.

[15] Now at The University of Melbourne, Victoria, Australia.

[16] Now at IPHE Université de Lausanne, CH-1015 Lausanne, Switzerland.

[17] Now at IEKP Universität Karlsruhe, Germany.

[18] Now at University of Antwerpen, Physics Department, B-2610 Antwerpen, Belgium; supported by Interuniversity Attraction Poles Programme—Belgian Science Policy.

[19] And High Energy Accelerator Research Organisation (KEK), Tsukuba, Ibaraki, Japan.

[20] Now at University of Pennsylvania, Philadelphia, PA, USA.

[21] Now at TRIUMF, Vancouver, Canada.

[22] Now at DESY Zeuthen.

[23] Now at CERN.

[24] Now at DESY.

✠ Deceased.

constraints of energy and momentum conservation are imposed [1]. An accurate determination of the LEP beam energy is therefore of paramount importance, since it sets the scale for the W mass measurement.

The standard approach used to determine the average beam energy at LEP II [2] involves precise measurements based on resonant depolarisation of the beams at energies in the range 41–61 GeV, combined with magnetic extrapolation to higher energies using NMR probe measurements. Corrections are applied to account for variations of the beam energy with time, and for differences at the four experimental interaction points around the ring. The LEP Energy Working Group calculates the beam energy for each experiment for periods of 15 minutes, or more frequently if a change in operating conditions causes an abrupt shift in the beam energy. The systematic uncertainty in the beam energy is dominated by the precision of approximately 10 MeV in the magnetic extrapolation and, uniquely in 2000, by the error of approximately 15 MeV associated with the strategy (so-called bending field spreading) to boost the beam energy to the highest possible value.

In this Letter we assume the modelling of variations in the LEP beam energy to be correct and perform a check on the overall energy scale using radiative return events of the type

$$e^+e^- \to Z\gamma, \quad Z \to f\bar{f},$$

where the fermion f is a quark, electron, muon or τ-lepton. Since the Z mass is very precisely known from LEP I [3], the kinematic properties of these events can be used to estimate the beam energy, which is assumed to be equal for the electron and positron beams. For hadronic events, information is taken from the jet energies and directions, while for leptonic events only the angular information is used.

The results of these measurements of the beam energy, using the information from observed events,

can be interpreted in several ways. Any discrepancy could indicate a problem with the LEP energy calibration. Alternatively, since the techniques employed are closely related to those used in the W mass measurement, they could be regarded as a check of detector systematic errors, or of hadronisation uncertainties in the case of hadronic events. The results could also be regarded as a check on the Monte Carlo modelling of initial-state radiation (ISR) in the radiative return process.

This Letter is organised as follows: a summary of the data and Monte Carlo samples used is given in Section 2, the analysis method is explained in Section 3 and the estimation of systematic errors is described in Section 4. Finally we summarise and discuss the results in Section 5.

2. Data and Monte Carlo samples

The OPAL detector,[25] trigger and data acquisition system are fully described elsewhere [4–8]. The data used for the present analysis were collected between 1997 and 2000, at centre-of-mass energies in the range from 183 GeV to 209 GeV. The approximate amount recorded at each nominal energy is given in Table 1.

Samples of Monte Carlo simulated events are used to interpret the data. Separate Monte Carlo samples were generated at each of the nominal centre-of-mass energy values considered and also at several intermediate points. The programs employed for this purpose are outlined below. First we give those used to generate signal events, then those for generation of the various backgrounds. All Monte Carlo samples were passed through the OPAL detector simulation program [9], and processed in the same way as real data.

For the hadronic final states, the KK2f [10] program (v.4.13) is used to generate the $q\bar{q}(n\gamma)$ process (where n is an integer), including the signal $q\bar{q}\gamma$ events, and likewise the $\mu^+\mu^-(n\gamma)$ and $\tau^+\tau^-(n\gamma)$ processes. In this scheme, ISR is modelled with Coherent Exclusive Exponentiation (CEEX) [11] to $\mathcal{O}(\alpha^2)$ precision. For the $e^+e^-(n\gamma)$ final-state process, BHWIDE [12] (v.1.00) is employed, in which ISR

---

[25] OPAL uses a right-handed coordinate system in which the z axis is along the electron beam direction and the x axis is horizontal. The polar angle θ is measured with respect to the z axis and the azimuthal angle ϕ with respect to the x axis.

Table 1
Nominal centre-of-mass energies and approximate integrated luminosities for data collected between 1997 and 2000

Year(s)	$\sqrt{s}$/GeV	$\int \mathcal{L}\,dt$/pb^{-1}
1997	183	58
1998	189	186
1999	192	30
1999	196	78
1999 + 2000	200	79
1999 + 2000	202	38
2000	205	82
2000	207	137
1999	192–202	223
2000	200–207	221

is modelled with YFS [13] exponentiation to $\mathcal{O}(\alpha)$ precision. For the hadronic final states, fragmentation of the primary quarks is performed according to the PYTHIA (v.6.150) [14] prescription, with HERWIG (v.6.2) [15] and ARIADNE (v.4.11) [16] employed for systematic studies. In order to simulate properly the interplay between photon and gluon radiation in the final-state parton shower, final-state radiation (FSR) of photons is turned *off* in the generation of the primary quark pairs in KK2f and turned *on* in the hadronisation programs. As a consequence, the Monte Carlo for hadronic events does not include the interference between initial- and final-state photon radiation (I/FSR interference) which is naturally present in the data. The absence of this is taken as a systematic uncertainty, as described in Section 4.1. For leptonic final states this problem does not arise and the Monte Carlo includes I/FSR interference.

Four-fermion backgrounds are simulated using grc4f [17] or KORALW [18] with matrix elements from grc4f, and two-photon backgrounds using PHOJET [19], PYTHIA, HERWIG, TWOGEN [20] and VERMASEREN [21]. For systematic studies of tau-pair backgrounds in the hadronic channel, the KORALZ [22] generator is also employed.

3. Analysis method

3.1. Hadronic channel

3.1.1. Event selection

The analysis in the hadronic final state closely follows the procedures used in the measurement of

hadronic cross-sections [23–27]—hadronic events are selected according to the same criteria and the effective centre-of-mass energy of the hadronic system after ISR, $\sqrt{s'}$, is computed by an identical algorithm. In summary, the algorithm to determine $\sqrt{s'}$ starts by identifying isolated photons in the electromagnetic calorimeter with energies greater than 10 GeV, based on their expected narrow lateral shower shapes and their lack of penetration into the hadronic calorimeter. The remaining tracks and clusters (in both electromagnetic and hadronic calorimeters) are formed into jets using the Durham algorithm [28] with a jet resolution parameter $y_{cut} = 0.02$. If more than four jets are found, a four-jet configuration is enforced nevertheless. A standard algorithm [29] is applied to reduce double counting of energy before calculating the jet energies, masses and directions. As was done for the W mass analysis [30], small corrections to the jet parameters and their errors are applied to improve the consistency between data and Monte Carlo, based on studies of Z calibration data and of full-energy events in the high energy data. A kinematic fit is performed to improve the estimates of the jet four-momenta by imposing the constraints of energy and momentum conservation. The rôle of the beam energy in this fit is elaborated on below. If this fit is unsuccessful, an additional unseen photon is assumed moving parallel to the beam direction (z), and the kinematic fit is repeated. If this fails, a fit involving two unmeasured photons in the $\pm z$ directions is attempted. The value of $\sqrt{s'}$ is obtained as the invariant mass of the jets resulting from the first successful fit. Events classified by the algorithm as having exactly one photon, either measured in the calorimeter or parallel to z, are retained for analysis; events classified as having multiple photons are discarded, suffering from poorer resolution on $\sqrt{s'}$ or higher background. The typical resolution on $\sqrt{s'}$ is around 2 GeV, though with tails associated with unresolved multiple soft photon radiation.

3.1.2. Fitting method and results

The reconstructed $\sqrt{s'}$ distributions of the data and Monte Carlo are compared for hadronic events in Fig. 1(a); the Z mass peak is clearly seen. The background to the $Z\gamma$ final state is around 4%, and is dominated by the $q\bar{q}e^+e^-$ four-fermion process in which the $q\bar{q}$ arise from the decay of a Z boson, so most of these events can also effectively be regarded

as signal. The calculation of $\sqrt{s'}$ relies on the constraint in the kinematic fit that the energies of the jets and photons add up to the centre-of-mass energy. In Monte Carlo events, the correct centre-of-mass energy is of course known a priori. In the case of data, we use the beam energies determined from the magnetic extrapolation method by the LEP Energy Working Group. Any systematic inaccuracy in this estimate of the beam energy would be manifested as a shift in the reconstructed Z peak in data. The basis of the analysis method is therefore to reconstruct $\sqrt{s'}$ in the data as a function of an assumed difference, ΔE_{beam}, between the real beam energy and that estimated from magnetic extrapolation, and to find the value of ΔE_{beam} which optimises the agreement between the peaks in data and Monte Carlo. The sign of ΔE_{beam} is such that a positive (negative) value implies that the value determined from OPAL data is higher (lower) than that determined by the LEP Energy Working Group.

To compare data and Monte Carlo, we fit an empirical analytic function to the Z mass peak for 26 bins in the region $87 < \sqrt{s'}/\text{GeV} < 100$ and characterise the distributions by the fitted peak position, M^*. The function chosen has the form

$$S(\sqrt{s'}) = A\left[c\left(\frac{2\sqrt{s}}{s-s'}\right)\frac{s'\Gamma_{\pm}^2}{(s'-M^{*2})^2 + s'\Gamma_{\pm}^2} + a\left(1 + b\sqrt{s'}\right)\right], \quad (1)$$

where

$$\Gamma_{\pm} = \begin{cases} \Gamma_-, & \text{for } \sqrt{s'} < M^*, \\ \Gamma_+, & \text{for } \sqrt{s'} > M^*. \end{cases}$$

It consists of two parts that, together, are found to fit the peak well. The first part describes the contribution of processes which are resonant at the Z peak, including the signal $q\bar{q}\gamma$ production. It comprises a pair of matched relativistic Breit–Wigner functions with different widths, Γ_- and Γ_+, below and above the peak respectively, and a normalisation factor, c. The factors of $\Gamma_{\pm}^2$ in the numerator ensure continuity of the function at $\sqrt{s'} = M^*$. The factor $\frac{2\sqrt{s}}{s-s'}$ is intended to represent the effect of a bremsstrahlung spectrum proportional to the reciprocal of the energy of an ISR photon, though it actually has a rather small effect. The second part describes the non-resonant background
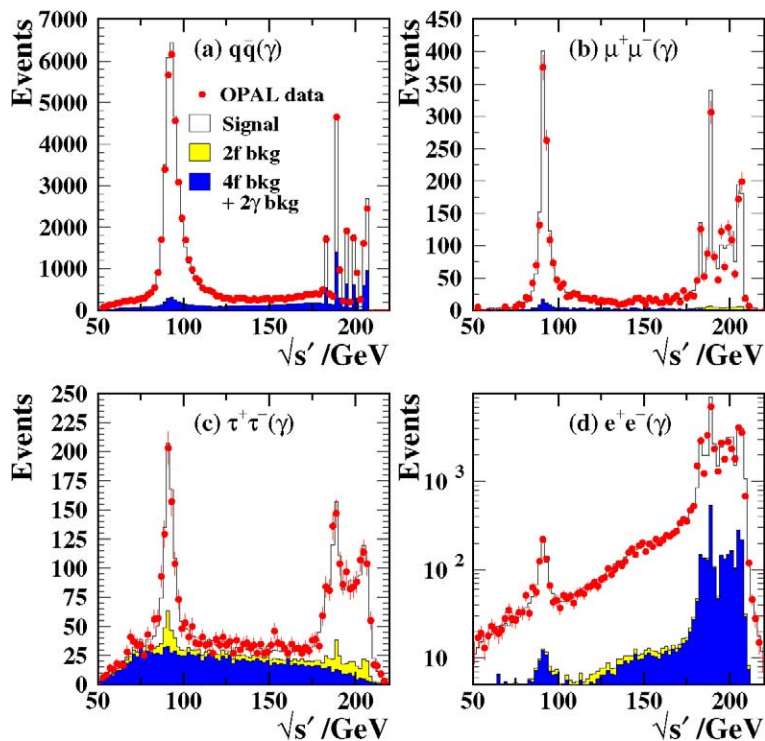
Fig. 1. Distributions of $\sqrt{s'}$ for (a) hadronic and (b)–(d) leptonic events before applying cuts on photon radiation. Data with centre-of-mass energies between 183 and 209 GeV have been combined. Full-energy events from data-taking at different centre-of-mass energies are responsible for the multiple peaks observed at high $\sqrt{s'}$. The corresponding Monte Carlo expectation is also shown, normalised to the integrated luminosity of the data. The Monte Carlo samples are not generated at exactly the same energies as the data, which together with binning effects explains the visible differences in structure for full-energy events. (The poorer resolution for tau-pair events washes out this effect.) The radiative return peak is dwarfed by the contribution from t-channel full-energy events for electrons.

contribution. It is a function linear in $\sqrt{s'}$, with a parameter, b, determining the shape and a parameter, a, providing normalisation. First of all the background parameters are extracted from fits to Monte Carlo simulations of two-photon and four-fermion (excluding $q\bar{q}e^+e^-$) events, which are non-resonant under the peak, at several centre-of-mass energies; their energy-dependences are taken from linear fits. The parameters $\Gamma_\pm$ and c are then extracted from fits to Monte Carlo, including both the resonant and the non-resonant contributions, at the same centre-of-mass energies, with the background parameters constrained to those previously determined; their energy-dependences are also taken from linear fits. Finally, in fitting the Monte Carlo and data with all parameters constrained to their energy-determined values, only the overall normalisation, A, and the peak position, M^*, are allowed to vary.

From the data recorded in the years 1997, 1998, 1999 and 2000, the numbers of selected events in the fit region are 2386, 7238, 7198 and 6300, respectively. Typical fits used to determine M^* in Monte Carlo and data are shown in Fig. 2. The method for estimating ΔE_{beam} is illustrated by Fig. 3, which shows the value of M^* obtained from the data as a function of the assumed value of ΔE_{beam}. The data points define a band of constant width, since the statistical errors are almost fully correlated from point to point. The fitted value of M^* in the Monte Carlo is evaluated for a range of generated beam energies; a weak dependence of about 10 MeV in M^* for a 1 GeV change in beam energy is observed. To account for this, as the beam energy (and hence ΔE_{beam}) is varied in the data, the corresponding value of M^* in data is compared with the expected value of M^* in Monte Carlo for a *known* beam energy in Monte Carlo corresponding to this *assumed* average
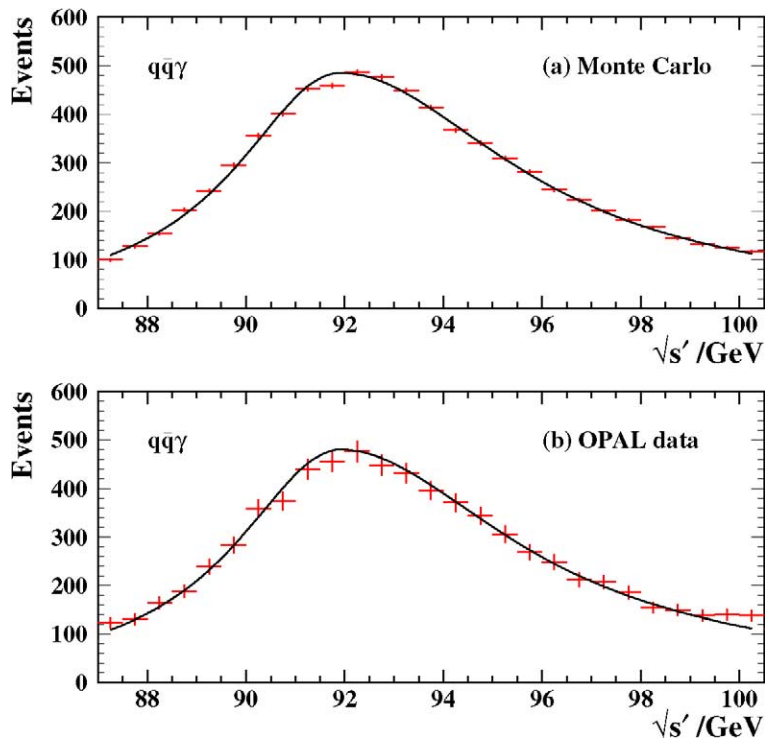
Fig. 2. Fits of Eq. (1) to (a) Monte Carlo generated at 189 GeV and (b) OPAL data collected in 1998, at the same nominal energy, for hadronic events. The Monte Carlo expectation is normalised to the integrated luminosity of the data.

beam energy in data. This is represented by the near-horizontal line. The point where this crosses the data therefore gives the estimated value of ΔE_{beam} in the data.

The values of ΔE_{beam} with their statistical errors are given in Table 2. The systematic errors are estimated as described in Section 4.1. Measurements on subsets of the data collected at the nominal energy points detailed in Table 1 are performed in an equivalent manner.

3.2. Leptonic channels

3.2.1. Event selection

Although the leptonic channels offer lower statistics than the hadronic final state, the systematic uncertainties associated with the measurement are different. Of the three lepton species, the muon sample gives the most precise result, benefitting from a very low background and an excellent angular resolution for the two muons. The tau channel suffers from lower selection efficiency, a worse resolution of the tau-lepton direction and a larger background. The situation for the electron channel is complicated by the t-channel exchange contribution. Nonetheless, this channel turns out to be more precise than the tau channel.

In general, the lepton-pair event selection looks for the two charged leptons, and possibly a photon in the detector. Photons are identified as clusters in the electromagnetic calorimeter with a narrow shower shape consistent with being a photon, no associated track and with energy greater than 5 GeV. Only the highest energy photon candidate is considered. In all cases the event is treated as having exactly three final-state particles, two leptons and a photon. If no photon is observed, then the third particle is taken to be a photon along the beam axis, recoiling against the two-lepton system. Events with an observed photon between 5 and 30 GeV are rejected because they would fall far away from the radiative return peak if there were only one final-state photon in this energy range. Events with an observed photon with energy greater than 30 GeV
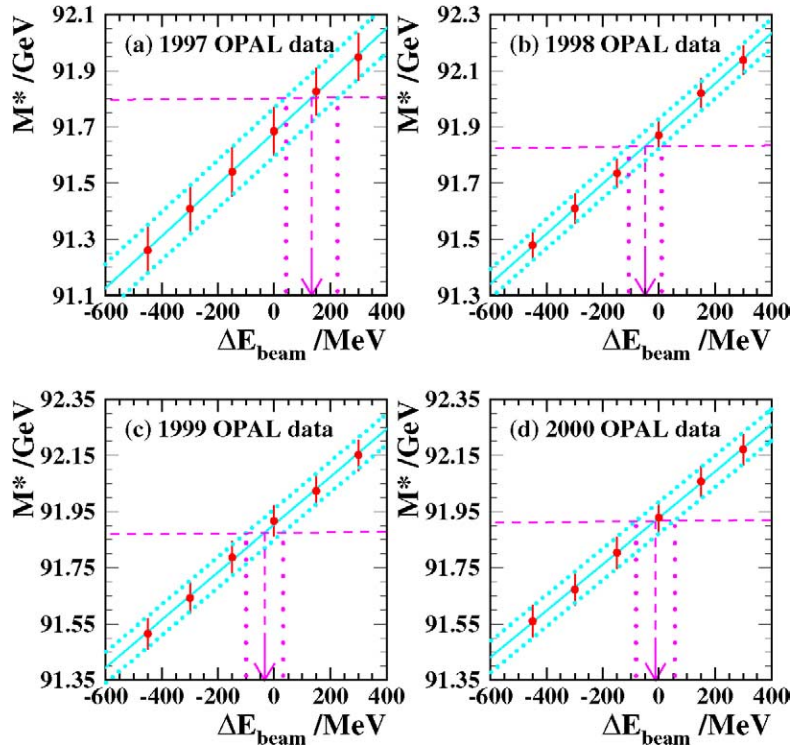
Fig. 3. Extraction of ΔE_{beam} from hadronic events in OPAL data collected during (a) 1997, (b) 1998, (c) 1999 and (d) 2000. Each plot shows the value of the peak position, M^*, obtained from data as a function of the assumed correction to the LEP beam energy, ΔE_{beam}. The solid line is a fit to the points, while the diagonal dotted lines define the statistical error band. The near-horizontal dashed line indicates the Monte Carlo expectation for M^* as a function of ΔE_{beam}. The intersection of this with the diagonal band allows the true value of ΔE_{beam} and its statistical error to be inferred from the data.

Table 2
Summary of the values of ΔE_{beam} derived from hadronic and leptonic events for each year and for all years combined. (For the statistically more precise hadronic channel, the results are also presented at the individual nominal energy points for data collected in the years 1999 and 2000.) In each case, the first error is statistical and the second systematic

Year	ΔE_{beam}/MeV				
	$q\bar{q}\gamma$	$\mu^+\mu^-\gamma$	$\tau^+\tau^-\gamma$	$e^+e^-\gamma$	All channels
1997	$+134 \pm 92 \pm 33$	$+577 \pm 251 \pm 29$	$+1157 \pm 548 \pm 89$	$-1590 \pm 589 \pm 86$	$+176 \pm 84 \pm 28$
1998	$-49 \pm 59 \pm 52$	$+71 \pm 133 \pm 30$	$+266 \pm 282 \pm 93$	$+172 \pm 217 \pm 75$	$+8 \pm 53 \pm 37$
192 GeV	$-103 \pm 123 \pm 30$	–	–	–	–
196 GeV	$-37 \pm 117 \pm 36$	–	–	–	–
200 GeV	$+35 \pm 113 \pm 37$	–	–	–	–
202 GeV	$-98 \pm 183 \pm 39$	–	–	–	–
205 GeV	$+4 \pm 106 \pm 68$	–	–	–	–
207 GeV	$-24 \pm 93 \pm 73$	–	–	–	–
1999	$-34 \pm 66 \pm 36$	$-71 \pm 131 \pm 28$	$+529 \pm 291 \pm 88$	$-271 \pm 270 \pm 70$	$-30 \pm 57 \pm 27$
2000	$-12 \pm 69 \pm 72$	$-293 \pm 165 \pm 33$	$+399 \pm 448 \pm 108$	$-393 \pm 303 \pm 73$	$-89 \pm 65 \pm 51$
All years	$+1 \pm 38 \pm 40$	$-32 \pm 75 \pm 25$	$+313 \pm 175 \pm 76$	$-88 \pm 146 \pm 46$	$0 \pm 34 \pm 27$

are assumed to have no radiation along the beam direction. The angles of all tracks, and of calorimeter clusters in the electron-pair events, are calculated taking into account the offset of the beam spot position from the nominal detector origin.

The planarity of the event is defined as the sum of the three angles between the directions of the two leptons, and the direction of the photon, either the observed photon in the detector or along the beam axis. The event planarity must be greater than 350°. True three-body events and events with only collinear initial-state radiation along the z-axis are planar, unlike events from four-fermion processes, for example.

The selection of muon events used here is the same as in Refs. [25–27], with the addition of the planarity cut defined above. A total of 3604 muon-pair events is selected in the combined 1997 to 2000 data, with 9% background according to the Monte Carlo. There are 1166 events in the radiative return peak region, defined by $82 < \sqrt{s'}/\mathrm{GeV} < 102$, with 6% background, dominated by four-fermion and two-photon processes.

Although the tau sample includes a larger background than the muon channel, background from other processes including Z decay to a fermion pair can be included in the signal, while background from two-photon and other four-fermion processes is flat under the radiative return peak. A dedicated tau selection is therefore used here, which is somewhat more efficient than that used in the OPAL two-fermion cross-section analyses, at the expense of including more background.

The tau selection excludes events which are identified as $e^+e^-(\gamma)$ or $\mu^+\mu^-(\gamma)$ candidates. Low multiplicity events are required, with at least 2 and not more than 6 tracks. The number of tracks plus the number of energy clusters in the electromagnetic calorimeter must be less than 16. The events are required to be consistent with originating from the beam collision in space and time to reject cosmic rays. A cone jet finding algorithm is applied, searching for cones of half angle 45°, each containing at least 5% of the centre-of-mass energy. At least two cones must be identified in the event. If only two cones are found, these are assumed to be τ-leptons, with an unobserved photon in the beam pipe. If three or more cones are found, then isolated photon candidates with energy greater than 5 GeV are also identified. The cone containing the highest energy photon candidate is taken to be the

photon when reconstructing the event. Of the remaining cones, the two with highest energy are taken to be the τ-leptons. If there are three or more cones but no identified photon, then the two highest energy cones are taken to be the τ-leptons, and the third most energetic cone is treated as an observed photon. Events where the "photon" cone has energy less than 30 GeV are then rejected.

The two tau cones must satisfy

$$|\cos\theta_{\mathrm{cone}}| < 0.9$$

to reduce the contamination from t-channel Bhabha events. The scalar sum of the energy in tracks and clusters (with no correction for double counting) divided by the centre-of-mass energy must be in the range

$$0.3 < \sum E/\sqrt{s} < 1.1.$$

Low energy events are predominantly from two photon events, and high energy events are overwhelmingly dominated by Bhabhas.

In the combined 1997 to 2000 data, 4173 events are selected in the data, which according to the Monte Carlo comprise 52% tau pairs, with an additional 12% of "resonant" background (i.e., electron-, muon- and quark-pair events). Under the radiative return peak, there are 973 events, and the purity increases to 59% tau pairs, with a further 12% resonant events. The average efficiency for selecting tau-pair events over all the centre-of-mass energies studied is 46%.

The selection of $e^+e^-(\gamma)$ events used here is almost entirely based on calorimeter information, motivated by avoiding systematic uncertainties in the modelling of forward, high-energy electron tracks. Low multiplicity events are required, with fewer than 18 tracks plus clusters, and events selected as muon pairs are excluded. Photon or electron-like clusters are identified in the electromagnetic calorimeter by applying the photon selection, but allowing tracks to be associated with the clusters. These clusters are sorted according to their energy. The two or three most energetic clusters must satisfy $E_1 + E_2 + E_3 > 0.7\sqrt{s}/2$ and $E_2 > 0.2\sqrt{s}/2$. The two highest energy clusters must be in the angular region $|\cos\theta_{\mathrm{clus}}| < 0.9$. The same scalar sum of energy in tracks and clusters as used above in the tau-channel selection must pass $\sum E/\sqrt{s} > 1.0$.

In the 1997 to 2000 data, a total of 47 775 events is selected. This number is overwhelmingly dominated

by nearly back-to-back t-channel exchange events, with only 825 events falling in the radiative return peak region. Under the peak, 1% of the events are from resonant backgrounds and 9% from other backgrounds, dominated by four-fermion and two-photon processes. (The s- and t-channel processes are not separated—all $e^+e^-(\gamma)$ final states count as "signal".)

3.2.2. Fitting method and results

Each leptonic event is assumed to contain exactly three final-state particles: two leptons plus one and only one photon. The ratio of s'/s is determined from the directions of these particles. The photon is assumed to travel along the beam axis, recoiling against the leptons, unless a photon candidate with energy greater than 30 GeV is observed in the detector, in which case the direction of the electromagnetic cluster is taken to be the photon direction. For muon-pair events, the directions of the muon tracks are used, and for tau pairs the directions of the cones, defined as the

vector sum of the tracks and clusters in the cone, without any correction for double counting. For electrons, the directions of the electromagnetic calorimeter clusters are taken. The only energy information used is the loose 30 GeV minimum energy requirement on an observed photon.

The ratio s'/s is given by

$$\frac{s'}{s} = \frac{\sin\alpha_1 + \sin\alpha_2 - |\sin(\alpha_1 + \alpha_2)|}{\sin\alpha_1 + \sin\alpha_2 + |\sin(\alpha_1 + \alpha_2)|}, \qquad (2)$$

where α_1 and α_2 are taken to be the polar angles $\theta_{1,2}$ of the two leptons in the detector if the photon is undetected, or the angles between the two leptons and the photon direction if the photon is detected. The distributions of $\sqrt{s'}$ are shown in Fig. 1(b), (c) and (d) for the muon, tau and electron samples, respectively. For genuine radiative return events, the value of $\sqrt{s'}$ is approximately equal to the mass of the Z boson.

As for the hadronic samples, the values of $\sqrt{s}$ for the data are those provided by the LEP Energy Work-
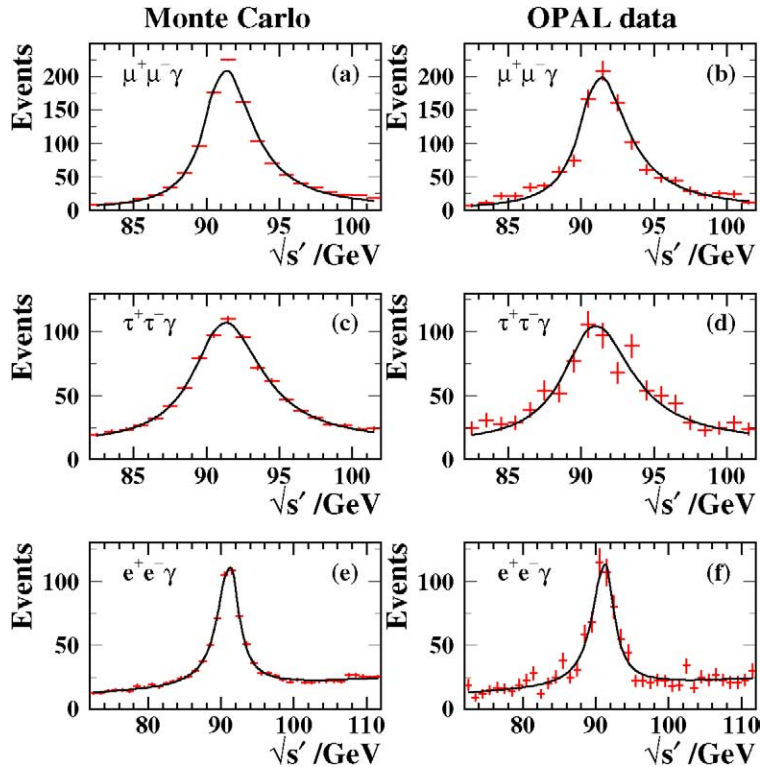

Fig. 4. Fits of Eq. (1) to Monte Carlo (left-hand plots), combining samples generated at energies in the range 183–209 GeV, and OPAL data (right-hand plots) collected in the years 1997–2000 at the same nominal energies, for muon-, tau- and electron-pair events, respectively. The Monte Carlo expectation is normalised to the integrated luminosity of the data in each case.

ing Group, while for the Monte Carlo sample, the true value is known exactly from the event generation. Fits are made to the $\sqrt{s'}$ distribution for 20 bins in the region $82 < \sqrt{s'}/\text{GeV} < 102$ for the muon and tau-pair samples, and 40 bins spanning 72 to 112 GeV for the electron-pair events, to allow the t-channel contribution to be constrained by the data. For muon and tau events, the same method is used as for hadrons, but with the parameter b in Eq. (1) set to zero so that the non-resonant background is assumed to be constant. For the electron sample, a first fit for the parameter a is made as before to the non-resonant background Monte Carlo samples alone. Then, when fitting the signal plus background, an additional linear term of the form $f(1 + g\sqrt{s'})$ is included to account for the t-channel contribution to the signal. The parameters f and g are similarly fixed from the Monte Carlo simulation. Data and Monte Carlo samples from all centre-of-mass energies are fitted together for the central result, allowing for no energy dependence of the parameters describing the background, the widths or the value of M^*. Separate fits are also made for data from each year of running, using Monte Carlo samples from the same range of centre-of-mass energies.

The variation of the position of the peak M^* in the Monte Carlo is evaluated as a function of a shift in the assumed beam energy ΔE_{beam}. This is used to convert the difference between the peaks in data and Monte Carlo into the difference between the beam energies observed in OPAL and provided by the LEP Energy Working Group. The results are given in Table 2, and the data quality is illustrated in Fig. 4.

Cross-checks are made using different fitting methods. Fits are made to the distribution of reconstructed centre-of-mass energy, found using Eq. (2), assuming that $s' \equiv M_Z$ in every event. The binned data and Monte Carlo distributions are also compared directly as a function of the beam energy offset, instead of using an empirical functional form. In each case consistent results are found.

4. Systematic errors

4.1. Hadronic channel

The evaluation of systematic errors closely follows the approach used in the measurement of hadronic

cross-sections [23–27]. The following effects are taken into account, and the uncertainties are summarised in Table 5.

• *Detector modelling*. The inputs to the kinematic fits which determine $\sqrt{s'}$ are the measured energies, masses and angles of jets and photons and their resolutions. For the measurement of the W mass [30], studies of calibration data taken at the Z peak are used to apply small corrections to these energies and angles in the Monte Carlo simulation in order to achieve agreement with the data. The same corrections, determined separately for each year of data-taking where appropriate, are applied in the present analysis. The errors in the correction factors are then taken to define systematic errors in the value of ΔE_{beam}. Of particular concern are potential systematic shifts in the reconstruction of the polar angular scale, θ, of jets (equivalent to an uncertainty in the effective length/radius ratio of the detector), as these could bias the reconstruction of $\sqrt{s'}$. These are assessed by comparing the jet angles in Z events reconstructed using tracking and calorimetry separately.

In addition, the effects of deviations from linearity in the jet energy scale of around $\pm 1\%$, going from ~ 20 to ~ 100 GeV, are corrected for and the error in the correction is taken as a further source of systematic uncertainty. This non-linearity is assessed from studies of three-jet events in Z decays and of full-energy hadronic events in the high energy data. The linearity of the photon energy scale is likewise studied using $e^+e^-\gamma$ and $\mu^+\mu^-\gamma$ events in both the Z calibration data and the high energy data. Though no significant deviations from linearity are seen in this case, the error in the determination of the linearity is similarly used to define a systematic uncertainty.

A further consideration is the uncertainty in the measured masses of jets. Studies of Z calibration data suggest that the relationship between the jet mass scales in Monte Carlo and data is correlated with the relationship between the respective jet energy scales. The likely size of any uncertainty in the measured jet masses is therefore assessed by rescaling these in proportion to the corrections applied to the jet energies described above. Whereas the true jet energies are known in Z calibration data and can therefore be corrected, the true jet masses are not. Consequently no corresponding corrections can be made for the jet

Table 3
Detector modelling systematic error contributions on ΔE_{beam} for hadronic events

Detector effect	Systematic error/MeV				
	1997	1998	1999	2000	All years
Jet mass scale	8	41	13	60	25
Jet energy scale	16	17	18	18	17
Photon energy scale	14	13	11	8	12
Jet angular scale	9	9	9	9	9
Photon angular resolution	2	3	5	7	4
Photon energy linearity	4	4	4	4	4
Photon energy resolution	2	3	4	6	3
Jet energy resolution	1	2	2	3	2
Jet energy linearity	< 1	1	1	1	1
ECAL energy scale	1	1	3	5	2
Jet angular resolution	< 1	< 1	1	1	< 1
Total	25	47	28	65	34

mass scale, while the full size of the shift seen when rescaling the jet masses is applied as a systematic uncertainty. As the scale factors are determined from independent calibrations for each year, the effect of this is strongly year-dependent.

The Z data are finally used to estimate the uncertainty in the simulation of the electromagnetic calorimeter energy scale in hadronic events, since the primary hadronic event selection relies on this.

The largest influence on ΔE_{beam} arises from the uncertainty in the mass scale of jets, with other notable contributions from uncertainties in the energy scales of jets and photons and the angular scale of jets. Table 3 details these.

• *Fragmentation*. The sensitivity of the measurements to the fragmentation modelling of quarks is estimated by comparing the PYTHIA program (based on a parton shower model and string hadronisation) with HERWIG (parton shower model and cluster hadronisation) and ARIADNE (colour-dipole model and string hadronisation). In all cases the input parameters to the models are optimised through studies of global event shape variables and particle production rates in calibration data taken at the Z peak [31,32]. To reduce statistical errors on this comparison, the same primary quarks generated with KK2f are fragmented according to each model in turn. The larger deviation from the PYTHIA prediction arises from the comparison with ARIADNE; the size of this deviation is assigned as a

systematic error. The multiplicity cuts in the hadronic event selection are also varied by ±1 unit to check the sensitivity to modelling of low multiplicity jets. This effect is negligible by contrast.

• *Fit parameters*. The parameters fixed in the fits: a, b, c and $\Gamma_\pm$, are varied by one standard deviation of their fitted values. For the first three of these, negligible shifts of the peak position, M^*, result. Although shifts of M^* of up to ~ 15 MeV are observed in the cases of the fitted widths, the change in Monte Carlo is almost exactly mimicked by the corresponding change in the data. Accordingly a systematic uncertainty is assigned based on the residual bias between Monte Carlo and data.

• *ISR modelling*. The KK2f Monte Carlo is used as the default model for the $q\bar{q}\gamma$ process since it has the most complete available modelling of the ISR process, corresponding to $\mathcal{O}(\alpha^2)$ with CEEX. The precision is degraded to correspond to $\mathcal{O}(\alpha)$ by a reweighting procedure to give an estimate of the accuracy of the description of ISR. Following the recommendation of Ref. [33], half of the difference observed between the two schemes is assigned as a systematic error, reflecting the effects of missing higher order terms in the perturbative expansion. Further tests are performed against the exclusive exponentiation (EEX) scheme [34] (the more primitive version of CEEX, formulated in terms of spin-summed/averaged differential cross-sections rather than in terms of the more fundamental spin amplitudes) at various orders. The results of all these checks, averaged over years, are detailed in Table 4 for comparison.

• *Backgrounds*. The uncertainty arising from the estimation of the four-fermion background is assessed by comparing samples generated using grc4f and KORALW. The difference between the two predictions has a negligible effect, as expected, since the largest component of this background, the Ze^+e^- final state, can be regarded as signal-like. The uncertainty from the untagged two-photon background is assessed by comparing samples generated using PHOJET and PYTHIA, from the tagged two-photon background by comparing a combination of samples generated by HERWIG and PHOJET with samples generated by TWOGEN, and from the $\tau^+\tau^-$ background by comparing samples generated using KK2f and KORALZ. These differences in prediction also have a negligible effect.

Table 4

Shifts in ΔE_{beam}, averaged over years, due to different treatments of ISR. For the hadronic channel, a systematic uncertainty is assigned as half of the difference between the CEEX2 (no I/FSR interf.) and CEEX1 (no I/FSR interf.) schemes; for the leptonic channels, half of the difference between the CEEX2 (I/FSR interf.) and CEEX1 (I/FSR interf.) schemes is taken

Scheme		Shift in ΔE_{beam}/MeV		
KK2f weight	Precision	$q\bar{q}\gamma$	$\mu^+\mu^-\gamma$	$\tau^+\tau^-\gamma$
CEEX2 (I/FSR interf.)	$\mathcal{O}(1, \alpha, L\alpha, L^2\alpha^2, L\alpha^2)$	–	default	default
CEEX1 (I/FSR interf.)	$\mathcal{O}(1, \alpha, L\alpha)$	–	$+1$	-13
CEEX0 (I/FSR interf.)	$\mathcal{O}(1)$	–	-11	$+3$
CEEX2 (no I/FSR interf.)	$\mathcal{O}(1, \alpha, L\alpha, L^2\alpha^2, L\alpha^2)$	default	-4	-4
CEEX1 (no I/FSR interf.)	$\mathcal{O}(1, \alpha, L\alpha)$	-7	-2	-20
EEX3 (no I/FSR interf.)	$\mathcal{O}(1, \alpha, L\alpha, L^2\alpha^2, L^3\alpha^3)$	-14	0	-5
EEX2 (no I/FSR interf.)	$\mathcal{O}(1, \alpha, L\alpha, L^2\alpha^2)$	-13	0	-5

• *I/FSR interference*. As explained in Section 2, the Monte Carlo for hadronic events does not include the interference between initial- and final-state photon radiation (I/FSR interference) which is naturally present in the data. To estimate the error introduced by the absence of this effect in Monte Carlo, alternative samples of events were generated with FSR and I/FSR interference turned *on* in the generation of the primary quark pairs in KK2f, and FSR turned *off* in their subsequent fragmentation, performed by PYTHIA. A reweighting procedure enables these events to be compared with the corresponding events should I/FSR interference have instead been absent. Though FSR is incorrectly treated in this manner, the effect cancels to some extent in comparing the weighted and unweighted events. In any case, the negligible difference observed indicates that this concern is not a problem.

• *Beam energy spread/boost*. The effect of the finite spread of energies in the beams is to provide an event-by-event boost to the events, corresponding typically to an rms spread of 250 MeV in the centre-of-mass energy. In addition, there is a small net boost of up to about 20 MeV at the OPAL interaction point, caused by asymmetries in the LEP radio frequency accelerating system [2]. The size and spread of this boost is consistent with the muon-pair data (see Section 4.2). The consequence of the first effect is investigated by applying a Gaussian-distributed boost with mean zero and rms 250 MeV to the Monte Carlo events, and of the second by applying a boost of 20 MeV to every event. The combined effect on ΔE_{beam} is found to be no more than 1 MeV.

Table 5

Systematic error contributions on ΔE_{beam} for hadronic events

Effect	Systematic error/MeV				
	1997	1998	1999	2000	All years
Detector modelling	25	47	28	65	34
Fragmentation	13	15	18	21	16
Fit parameters	4	1	5	4	3
ISR modelling	3	3	3	4	3
Backgrounds	1	1	1	2	1
I/FSR interference	2	1	1	< 1	1
Beam energy spread/boost	1	1	< 1	1	1
Total	29	50	33	69	38
Monte Carlo statistics	12	10	7	7	5
LEP calibration	10	11	12	20	11
Full total	33	52	36	72	40

• *Monte Carlo statistics*. The uncertainty resulting from limited Monte Carlo statistics is regarded as a systematic error, but is quoted separately.

• *LEP calibration*. The error in the standard LEP determination of the beam energy [2] contributes to the uncertainty in the difference between this and the value determined from OPAL data. Being unassociated with the details of our method, it is quoted separately and is different in each year.

As a cross-check on the $\sqrt{s'}$ evaluation procedure, two alternatives are adopted. First, a simpler algorithm is used in which *exactly* one ISR photon, either in the calorimeter or along the z-axis, is allowed for *all* events. Second, an alternative set of cuts to identify photons in the calorimeter is applied to the default al-

Table 6
Systematic error contributions on ΔE_{beam} for leptonic events

Effect	Systematic error/MeV		
	$\mu^+\mu^-\gamma$	$\tau^+\tau^-\gamma$	$e^+e^-\gamma$
Lepton angular scale	21	66	24
Lepton angular resolution	2	4	7
Fit parameters	1	4	10
Non-resonant background	< 1	6	4
Bhabha/t-channel	< 1	3	5
ISR modelling	1	7	10
Beam energy spread/boost	2	5	6
Total	21	67	30
Monte Carlo statistics	9	34	34
LEP calibration	11	11	11
Full total	25	76	46

gorithm. Both give results consistent with the default; no further error is therefore assigned.

4.2. Leptonic channels

The following effects are taken into account, and the uncertainties are summarised in Table 6.

• *Lepton angular scale*. The measurement is sensitive to any bias in the reconstructed direction of tracks, clusters or cones, in particular the θ measurement (since the majority of events are those with the photon along the beam direction).

The analysis for the muon events is repeated using the measured θ value of the associated electromagnetic energy cluster (shift of $+24$ MeV in ΔE_{beam}) or track segment in the muon chamber (shift of $+41$ MeV). These shifts are consistent with the rms shift estimated by an approximate Monte Carlo study, in which the track θ measurement is shifted and smeared according to the mean and rms of the differences seen in data between the default track measurement and the alternative calorimeter or muon chamber measurement. The position of lead-glass blocks in the calorimeter is determined by the known geometry and survey information, and is independent of the tracking. There are known problems with modelling the energy deposition and apparent angle of minimum ionising particles especially in the endcap lead-glass. The track measurement can therefore be considered more reliable. The barrel muon chambers are partly calibrated against tracks, while the information from the end-cap

muon chambers is more independent. A systematic error of 21 MeV is assigned, equal to half of the larger shift seen, i.e., resulting from the comparison of tracking and muon chamber information.

The θ angle of the tau cone is reevaluated using tracks only (shift of $+131$ MeV) or clusters only (-22 MeV). A similar Monte Carlo study to that for the muon events confirmed that the shifts are consistent with the statistical uncertainty associated with the degradation in precision expected from removing clusters or tracks from the angle determination. A systematic uncertainty of 66 MeV is assigned, equivalent to half the larger shift.

Similarly, the θ angle of electron candidates is replaced by the direction of the associated track (shift of -48 MeV). There is a problem with the modelling of high energy, fairly forward electron tracks, since electrons tend to radiate in the tracking volume, unlike muons. Again, half the shift, 24 MeV, is assigned as the systematic uncertainty.

• *Lepton angular resolution*. The modelling of the θ resolution is checked by examining the distribution of $\cos\theta_1 + \cos\theta_2$ for full-energy, back-to-back events. For muon and electron events, the resolution in data is worse than in the Monte Carlo, while for tau events the Monte Carlo resolution is slightly worse than that of the data. Part of the disagreement could be accounted for by the spread in centre-of-mass energy described below. The z-momentum in the Monte Carlo is smeared so as to bring the muon and electron distributions into agreement with the data, and by a similar amount in the tau-channel to estimate the systematic uncertainty.

• *Fit parameters*. The widths of the Breit–Wigner distribution are varied by their fitted errors, and the positions of the M^* peaks in data and Monte Carlo redetermined.

• *ISR modelling*. To evaluate the sensitivity to the modelling of ISR, the analysis is repeated, reweighting the KK2f Monte Carlo samples to other schemes. Samples of muon and tau pairs with event weights for the different schemes are available at 189 and 206 GeV. The CEEX scheme sometimes fails for muon events, in which case the EEX3 scheme is used. Very large weights are sometimes generated for tau events with a low tau-pair mass; weights larger than 10.0 are taken to be equal to 10.0. As can be seen in Table 4, the tau events show larger shifts than the

muon sample. Following the recommendations described above for the hadrons, half the difference between the CEEX2 and CEEX1 models (with interference between initial- and final-state radiation for leptons) is taken as a systematic uncertainty, i.e., $+1$ MeV and -7 MeV for the muon and tau events, respectively. The BHWIDE Monte Carlo is used for the electron channel, with calculations of order $\mathcal{O}(\alpha)$ with YFS exponentiation. Reweighting events to switch off the exponentiation, a shift of 4 ± 20 MeV is observed, where the error is statistical. An uncertainty of 10 MeV is assigned, equal to half the precision of this test.

• *Backgrounds*. Varying the small background in the muon sample has a negligible effect on the result. The two-photon, four-fermion and Bhabha backgrounds in the tau sample are each varied by $\pm 10\%$. This range is motivated by the discrepancies in the number of events below and above the $\sum E/\sqrt{s}$ range accepted in the tau event selection. The non-resonant background in the electron sample is also varied by $\pm 10\%$, and the rate and slope of the fitted t-channel contribution are shifted by the fitted errors.

• *Beam energy spread/boost*. The mean and width of the distribution of $\cos\theta_1 + \cos\theta_2$ for non-radiative Monte Carlo simulated muon-pair events is in reasonable agreement with the data when an average boost of 20 MeV with an rms spread of 250 MeV is applied to the simulation. The changes in ΔE_{beam} from applying these boosts to the simulation are assigned as a systematic uncertainty.

• *Monte Carlo statistics*. The uncertainty resulting from limited Monte Carlo statistics is regarded as a systematic error, but is quoted separately.

• *LEP calibration*. The error in the standard LEP determination of the beam energy [2] contributes to the uncertainty in the difference between this and the value determined from OPAL data. Being unas-
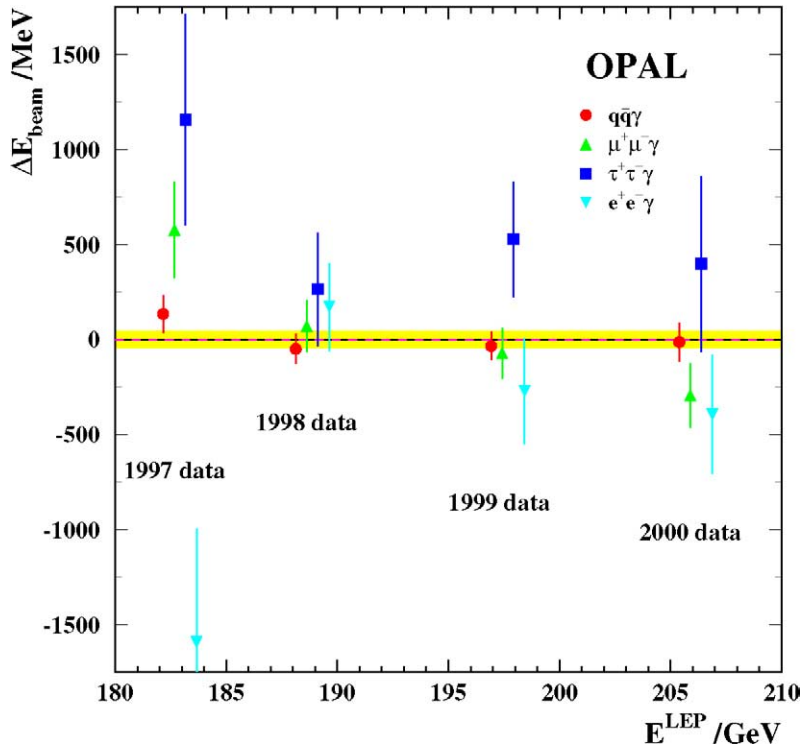

Fig. 5. Summary of measured values of ΔE_{beam}, using hadronic and leptonic events in OPAL data, as a function of the centre-of-mass energy. For clarity, measurements made with hadrons have been displaced leftwards by 0.5 GeV, while those made with tau and electron pairs have been displaced rightwards by 0.5 and 1.0 GeV, respectively. The dashed line represents the overall average, with the shaded band indicating its total error, including the 11 MeV uncertainty from the standard LEP beam energy determination.

sociated with the details of our method, it is quoted separately, averaged over years.

Tests with low statistics Monte Carlo samples give no indication of a bias in the method, and suggest that the errors from the fits are reasonable.

5. Discussion and summary

Using fermion-pair events at LEP II which exhibit radiative return to the Z, together with knowledge of the Z mass, we have made estimates of the LEP beam energy using OPAL data. In Fig. 5 we show a summary of the measurements of ΔE_{beam} using hadronic and leptonic final states at centre-of-mass energies from 183 to 209 GeV. There is no significant evidence for any dependence on centre-of-mass energy. Average values for each channel, and for each year of data-taking, are summarised in Table 2. Common systematic uncertainties are taken into account in forming the averages. For example, detector systematics for the hadron results are taken to be fully correlated from year to year, as are fragmentation systematics. However, detector systematics are assumed not to be correlated between hadrons and leptons, nor between different lepton species. The combined value for all energies from hadronic events is

$$\Delta E_{\text{b}} = +1 \pm 38(\text{stat.}) \pm 40(\text{syst.}) \text{ MeV},$$

while from leptonic events this is

$$\Delta E_{\text{b}} = -2 \pm 62(\text{stat.}) \pm 24(\text{syst.}) \text{ MeV}.$$

Both are evidently consistent with zero.

If all the results are combined, weighting the measurements using the total errors, and assuming the systematic errors to be uncorrelated between the hadronic and leptonic channels except for those associated with ISR modelling, the beam energy spread and boost and, in part, the LEP calibration, the overall estimate of the shift in the beam energy is

$$\Delta E_{\text{b}} = 0 \pm 34(\text{stat.}) \pm 27(\text{syst.}) \text{ MeV}.$$

The uncertainty from the standard LEP beam energy determination contributes 11 MeV to the systematic error.

We therefore see no evidence of any disagreement between the OPAL data and the standard LEP energy calibration, either overall or in any year of data-taking. Combination with similar results from other LEP experiments [35] should allow a more precise comparison with the beam energy determined by LEP.

References

[1] A. Ballestrero, et al., Physics at LEP2, CERN 96-01, vol 1, p. 141.
[2] LEP Energy Working Group, A. Blondel, et al., Eur. Phys. J. C 11 (1999) 573;
LEP Energy Working Group, R. Assmann, et al., CERN-PH-EP/2004-032, Eur. Phys. J., submitted for publication.
[3] Particle Data Group, K. Hagiwara, et al., Phys. Rev. D 66 (2002) 010001.
[4] OPAL Collaboration, K. Ahmet, et al., Nucl. Instrum. Methods A 305 (1991) 275.
[5] S. Anderson, et al., Nucl. Instrum. Methods A 403 (1998) 326.
[6] M. Arignon, et al., Nucl. Instrum. Methods A 313 (1992) 103;
M. Arignon, et al., Nucl. Instrum. Methods A 333 (1993) 330.
[7] J.T.M. Baines, et al., Nucl. Instrum. Methods A 325 (1993) 271;
D.G. Charlton, F. Meijers, T.J. Smith, P.S. Wells, Nucl. Instrum. Methods A 325 (1993) 129.
[8] OPAL Collaboration, G. Abbiendi, et al., Eur. Phys. J. C 14 (2000) 373.

[9] OPAL Collaboration, J. Allison, et al., Nucl. Instrum. Methods A 317 (1992) 47.

[10] S. Jadach, B.F.L. Ward, Z. Wąs, Comput. Phys. Commun. 130 (2000) 260.

[11] S. Jadach, B.F.L. Ward, Z. Wąs, Phys. Rev. D 63 (2001) 113009.

[12] S. Jadach, W. Placzek, B.F.L. Ward, Phys. Lett. B 390 (1997) 298.

[13] D.R. Yennie, S.C. Frautschi, H. Suura, Ann. Phys. (N.Y.) 13 (1961) 379.

[14] T. Sjöstrand, et al., Comput. Phys. Commun. 135 (2001) 238.

[15] G. Corcella, et al., J. High Energy Phys. 0101 (2001) 010.

[16] L. Lönnblad, Comput. Phys. Commun. 71 (1992) 15.

[17] J. Fujimoto, et al., Comput. Phys. Commun. 100 (1997) 128.

[18] S. Jadach, et al., Comput. Phys. Commun. 119 (1999) 272.

[19] R. Engel, J. Ranft, Phys. Rev. D 54 (1996) 4244.

[20] A. Buijs, et al., Comput. Phys. Commun. 79 (1994) 523.

[21] J.A.M. Vermaseren, Nucl. Phys. B 229 (1983) 347.

[22] S. Jadach, B.F.L. Ward, Z. Wąs, Comput. Phys. Commun. 79 (1994) 503.

[23] C.G. Ainsley, Studies of $Z/\gamma \rightarrow q\bar{q}$ events with the OPAL detector at LEP II, PhD thesis, University of Cambridge, RAL-TH-2003-001, January 2003.

[24] OPAL Collaboration, G. Abbiendi, et al., Eur. Phys. J. C 33 (2004) 173.

[25] OPAL Collaboration, G. Abbiendi, et al., Eur. Phys. J. C 13 (2000) 553.

[26] OPAL Collaboration, G. Abbiendi, et al., Eur. Phys. J. C 6 (1999) 1.

[27] OPAL Collaboration, K. Ackerstaff, et al., Eur. Phys. J. C 2 (1998) 441.

[28] S. Catani, et al., Phys. Lett. B 269 (1991) 432.

[29] OPAL Collaboration, G. Abbiendi, et al., Eur. Phys. J. C 26 (2003) 479.

[30] OPAL Collaboration, G. Abbiendi, et al., Phys. Lett. B 507 (2001) 29.

[31] OPAL Collaboration, G. Alexander, et al., Z. Phys. C 69 (1996) 543.

[32] OPAL Collaboration, G. Abbiendi, et al., Eur. Phys. J. C 35 (2004) 293.

[33] Reports of the Working Groups on Precision Calculations for LEP2 Physics: Two-fermion production in electron–positron collisions, CERN-YR-2000-009, hep-ph/0007180.

[34] S. Jadach, B.F.L. Ward, Comput. Phys. Commun. 56 (1990) 351.

[35] ALEPH Collaboration, R. Barate, et al., Phys. Lett. B 464 (1999) 339;
L3 Collaboration, P. Achard, et al., Phys. Lett. B 585 (2004) 42.